Egyptian Journal of Radiology and Nuclear Medicine

RESEARCH

Open Access

Additive value of fetal MRI to different ultrasound modalities in diagnosis of fetal GIT and abdominal wall anomalies

Hoda Magdy Abbas[1*], Soha Talaat Hamed[1], Hassan Mostafa Gaafar[2], Maha Mohammed Amer[1] and Safia Badr Sayed[1]

Abstract

Background Fetal MRI is a valuable supplementary study to the prenatal US in accurate diagnosis of fetal gastrointestinal anomalies and ventral abdominal wall anomalies, which has an impact on the postnatal outcome.

Aim of work To establish the additive role of fetal MRI to the prenatal US in the identification of complex fetal GIT anomalies.

Methods This prospective study involved 36 pregnant patients with age range from 19 to 41 years (mean ± SD of 27.8 ± 5.3 years). Thirty-six fetuses (19 males and 17 females). All cases underwent dedicated 2D obstetric ultrasound assessment with a focus on the fetal abdomen and some cases required additional 3D and 4D assessment. Twenty-seven patients underwent fetal MRI procedures.

Results In our study, fetal MRI was significantly more accurate than US in the confirmation and accurate delineation of the level of small bowel obstruction and differentiation of complete obstruction from luminal stenosis. In cases of anorectal malformations, prenatal US and fetal MRI were equally sensitive in the detection of their associated findings. While fetal MRI was superior to the US in the case of congenital chloride diarrhea. MRI images added the presence of distended oropharynx in esophageal atresia cases while other findings were detected with the same accuracy with both US and MRI. In cases of ventral abdominal wall defects, fetal MRI added fine details about the true size of the defect, the actual content of the abdominal wall defect as well as the detection of the presence of large bowel loops and related complications. In the category of fetal abdominal cysts, fetal MRI was superior to the US owing to its greater soft tissue characterization. In the case of sacrococcygeal teratoma (SCT), fetal MRI detected an additional intra-pelvic extension upgrading the tumor and detecting the true size of the intra-spinal component. In the category of congenital diaphragmatic hernia, MRI was superior in the detection of hernia capsule, herniated liver, and associated complications as well as accurate estimation of fetal lung volume. Studying the cases of cloacal malformations showed that owing to better tissue characterization by MRI the anomaly and its associated abnormal genitourinary communication were better delineated by MRI. The sensitivity of MRI to detect congenital anomalies concerning postnatal findings was 100%, the specificity was 50% and diagnostic accuracy was 96.6%. The sensitivity of ultrasound to detect congenital anomalies concerning postnatal findings was 85.3%, the specificity was 89%, and diagnostic accuracy was 80.6%. The sensitivity of combined US and MRI to detect congenital anomalies concerning postnatal findings was 100%, the specificity was 89%, and diagnostic accuracy was 93.1%.

*Correspondence:
Hoda Magdy Abbas
dr.hoda.magdy@hotmail.com
Full list of author information is available at the end of the article

Conclusions Fetal MRI is a valuable supplementary study to the prenatal US in accurate diagnosis of fetal obstructive gastrointestinal anomalies, ventral abdominal wall anomalies, fetal abdominal cysts, masses, and congenital diaphragmatic hernia**.** Fetal MRI is equally sensitive to the prenatal US in anorectal malformations.

Keywords Fetal MRI, Prenatal US, Fetal GIT anomalies

Background

Organs of the gastrointestinal tract, kidneys, urinary tract, suprarenal glands, and genitalia are all affected by congenital malformations. During the abnormalities screening ultrasound examination, aberrant pictures or the absence of normal structures are used to diagnose fetal abdominal malformations. Therefore, it is extremely important to collect and record standard normal photographs of the abdomen [1].

Congenital abdominal abnormalities can be detected in utero, and this has been shown to affect the baby's postnatal course (improved delivery planning, quicker surgical intervention, and fewer frequently occurring metabolic problems) [2].

For many years, ultrasound (US) has been the main imaging technique for fetal anomaly prenatal diagnosis [3]. The use of fetal MRI to visualize prenatal structures and the fetus in utero in detail is growing. However, only a small number of radiologists and doctors are conversant with fetal MRI. [4]. Usually, 1.5 T is used for fetal MRI. A field strength of 3 T is regarded as safe at any stage of gestation, while higher field strengths have also been employed [5].

The relative worth of US and MRI will keep changing as a result of continual technological advancement and clinical evaluation of both modalities' advancements. Prenatal diagnosticians currently have to decide which imaging modality to use to respond to particular clinical queries [2].

There are not many papers on the utility of MR imaging in prenatal abdominal diseases, which underlines the need for more extensive research to establish the function and worth of fetal abdomen MR imaging. We provide our knowledge of fetal MR imaging of abdominal abnormalities in this paper. This research aimed to establish the role of fetal MRI as a tool supplementary to prenatal US in the diagnosis of fetal GIT and abdominal wall anomalies, thus aiding in perinatal management and improving postnatal survival rates.

Patients and methods

This prospective study involved 36 fetuses (19 males and 17 females). All of the cases presented with suspected fetal GIT anomaly and were referred from the gynecology outpatient clinic, fetal medicine unit, and women's imaging unit for fetal MRI. The study was conducted at our university from October 2019 to March 2022. All of the study participants gave informed written consent to the study.

Inclusion Criteria: Pregnant patients with suspected fetal abdominal anomalies by antenatal ultrasound. Exclusion Criteria: a. pregnant patients with claustrophobia. b. Implants with electronic, magnetic, and mechanical components. c. Active devices with ferromagnetic or electronic controls, such as automatic cardioverter defibrillators. d. Artificial heart valves or pacemakers for the heart.

All patients were subjected to

a. Thorough clinical examination with history taking, and gynecological examination.
b. All cases underwent dedicated 2D obstetric ultrasound assessment with a focus on the fetal abdomen and some cases required additional 3D and 4D assessment using (Toshiba Aplio 550, trans-abdominal approach was done using 3–4 MHz).
c. Twenty-seven patients underwent fetal MRI procedures (MRI examination not done for all the studied pregnant patients due to technical difficulty and refusal of the patients) using two Philips medical systems devices (Entera and Achieva), which each used a 1.5-T magnet and a torso coil Table 1. MRI technique was used in this study.

Both MRI and US examinations were interpreted by two different expert radiologists, with more than 20 years of experience in each.

Statistical analysis and sample size

SPSS (statistical software for social science) version 26.0 was used to analyze the data on an IBM -compatible computer (SPSS Inc., Chicago, IL, USA). The accuracy of the qualitative data was evaluated using 2*2 contingency table equations of assessing the validity. The qualitative data were given as numbers and percentages "n (%)" [6]. The calculated sample size is 31 fetuses with GIT and abdominal wall abnormality. This number will be large enough to detect at least 3% (±6%) of GI tract abnormalities with MRI [2], at a 95% level of confidence and an 80% power of the study. This number will be increased by

Table 1 MRI techniques used in our study

Fetal MRI Protocol	
Survey BFFE)	TE 1.0 TR 3.0
FOV	250-350
T2 (TSE) Axial, coronal, and sagittal planes	TR 5025 TE 100
T1 TFE Axial, coronal and sagittal planes	TR 10 TE 5
T1 FSE breath hold.	TE 10.1-22.3 TR 300-700
BSSP; axial, coronal, and sagittal planes	TE 2.2 TR 4.2

10% to compensate for possible dropouts, and then the final sample size will be 35 fetuses.

Postnatal outcome

After imaging data were conducted, all cases were followed up in our obstetrics clinic for determination of the date and method of delivery or termination. Postnatal imaging in live births and autopsy in stillbirths and intrauterine fetal death (IUFD) were used as the gold standard for definite diagnosis and correlated with a diagnostic accuracy of Prenatal US and fetal MRI.

Results

This study was conducted on 36 pregnant patients ages ranging from 19 to 41 years (mean ± SD of 27.8 ± 5.3 years). The studied babies included 17 females (47.2%) and 19 males (52.8%). About 30.6% of our studied pregnancies ended with termination, while 25% underwent normal delivery at GA 37–39 weeks, and the rest 44.4% delivered by CS at 32–39 weeks. The outcome was live birth in 44.4% of the cases, stillbirth in 33.3%, and IUFD in 22.3%.

Those fetuses were examined by both ultrasonography (US) and magnetic resonance imaging (MRI) to detect their specificity and sensitivity of them in correlation to postnatal imaging or autopsy in the detection of abdominal anomalies.

Fetal abdominal anomalies in descending order of frequency were encountered in our study as follows:

a. Fetal obstructive esophageal and gastrointestinal anomalies in 18 cases (50%).
b. Fetal ventral abdominal wall defects in 7 cases (19.4%).
c. Fetal congenital diaphragmatic hernia in 6 cases (16.7%).
d. Fetal pelvi-abdominal cysts and masses in 5 cases (13.9%).

In our study, cases with suspected obstructive esophageal and gastrointestinal anomalies were displayed as follows; included four cases of small bowel obstruction, three cases with an anorectal malformation, and two cases of esophageal atresia.

In instances of small bowel obstruction

Fetal small bowel obstruction was prenatally diagnosed by the presence of three major US findings, namely the presence of dilated stomach, a dilated segment of small bowel loops, and polyhydramnios Fig. 1. On the other hand, fetal MRI was significantly more accurate than US in confirmation and accurate delineation of the level of small bowel obstruction and differentiation of complete obstruction from luminal stenosis owing to its ability to detect high T1 meconium signals (MR colonography) as follows:

a. One case with jejunal atresia: The prenatal US proposed the level of obstruction at the jejunoileal junction with distal collapsed small ileal loops. Based on

(See figure on next page.)

Fig. 1 A 28-year-old pregnant female with a follow-up 4D US reveling fetal small bowel dilatation. Ultrasound findings: **A**, **B** axial sections of the fetal abdomen showing borderline fetal small bowel dilatation with a maximum diameter of 14 mm. **C** axial section revealing a normal caliper colon. (**D**) images showing a normal AFI of 14.6 cm^3. MRI Findings: **E** Coronal, **F** axial T2WIs showing borderline fetal small bowel dilatation up to distal ileal loops in the left iliac region with the normal position of duodenojejunal flexure. **G**, **H**, **I** coronal T1WIs show an average caliper fetal whole colon down to the normal anorectal junction. **J** Postnatal fetal erect abdominal X-ray showed no air-fluid levels and the infant passed meconium combined US and MRI Diagnosis: Distal ileal stricture rather than atresia. Termination by CS at GA 39 weeks

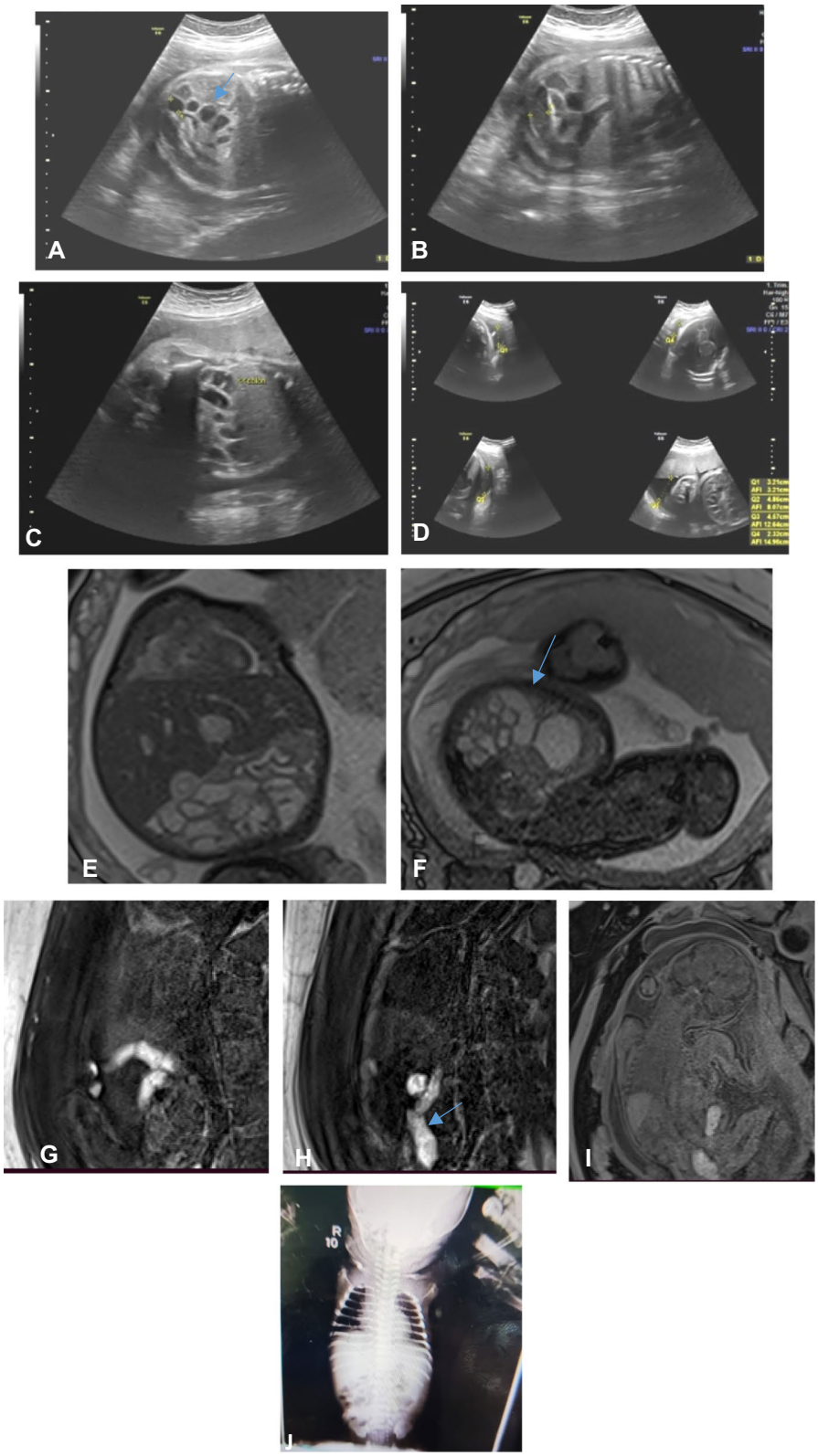

Fig. 1 (See legend on previous page.)

MRI, T2 WIs confirmed the site of the transitional zone, and T1WI added the presence of diminished meconium signals within distal ileal loops and the whole colon suggesting complete jejunal obstruction. Such a case ended with IUFD and the postnatal autopsy showed complete distal jejunal atresia.

b. One case with ileal atresia: The prenatal US detected increased fetal abdominal circumference by virtue of multiple dilated small bowel loops with a collapsed colon. On the other hand, T2WIs confirmed the level of obstruction, and T1WIs added the presence of an averagely distended fetal colon with a normal amount of fetal meconium up to the level of anorectal junction excluding the presence of multiple stenotic bowel segments. The infant was born by emergency CS with a markedly distended abdomen and postnatal US images confirmed the diagnosis.
c. One case with proximal ileal obstruction: Follow-up prenatal 4D US in scanning at the third trimester showed mildly dilated proximal ileal loops with no evidence of polyhydramnios or dilated stomach suggesting ileal stenosis versus malrotation. T2WIs detected the same US findings and excluded malrotation by the normal position of the duodenojejunal junction, and T1WIs added the presence of well-distributed meconium in distal ileal loops and whole colon suggesting incomplete ileal obstruction. The fetus was delivered by normal vaginal birth at 36 weeks and an immediate postnatal erect abdominal X-ray showed no air-fluid levels. Later on, that infant passed meconium excluding small bowel obstruction.
d. One case with duodenal obstruction: in which advanced prenatal US detected typical two bubble sign of dilated stomach and duodenum with severe polyhydramnios. Unfortunately, IUFD occurred before fetal MRI was done. The postnatal autopsy revealed a markedly distended fetal abdomen with complete duodenal obstruction.

In suspected anorectal malformation cases Fig. 2

Prenatal US showed a distended fetal abdomen with dilated bowel loops up to the level of anorectum as well as severe polyhydramnios with one case showing echogenic well-defined structures within the distended rectum (enterolith) suggesting the presence of a recto-vesical fistula. T2 WIs confirmed the presence of dilated fluid-filled small and large bowel loops and polyhydramnios as well as the presence of enterolith in one case appearing as low signal well-defined intra-luminal structures within the distended rectum. T1WI was very helpful as it detected reduced caliber and meconium signals at the site of rectal atresia in two cases and surprisingly the absence of meconium in one case suggesting the diagnosis of congenital chloride diarrhea (CCD) rather than an anorectal malformation. The case with suspected anal atresia with recto-vesical fistula ended with IUFD and autopsy confirmed the diagnosis. Other cases with suspected anorectal malformation were born by emergency CS with postnatal imaging confirming the diagnosis. The MRI suggested a case of CCD was born by elective CS with postnatal US showing dilated small and large bowel loops and the infant had severe watery diarrhea, confirming the diagnosis.

In suspected esophageal atresia cases

Prenatally, both US and T2WIs showed persistent small-sized fetal stomach in presence of polyhydramnios, T2 sagittal MRI images added the presence of a distended oropharynx in one out of 2 cases. Yet both US and MRI failed to identify the proximal esophageal pouch in the fetal neck (pouch sign). One case was born as stillbirth and an autopsy was not done, and another case was born living with postnatal gastrografin swallow confirming the diagnosis.

In the study of ventral abdominal wall defects

The results of the prenatal advanced 4D US of these cases were reported as follows; four cases of body stalk anomaly, one case of Gastroschisis, one case of Omphalocele, and one case of ruptured Omphalocele. Fetal MRI was done for only two cases, namely the Omphalocele and Gastroschisis cases. The other five cases underwent termination soon after diagnosis by advanced 4D US, so fetal MRI was not conducted.

In our study, cases with body stalk anomaly were diagnosed solely by advanced prenatal US by compilation of findings detected in all eight cases in form of large ventral abdominal wall defect with herniation of liver and small bowel loops being adherent to the amniotic membrane with associated very short umbilical cord, severe bowing, and angulation as well as shortening of fetal limbs with kyphoscoliosis of the fetal spine. The two cases with ruptured Omphalocele were suspected by the advanced US due to herniation of the liver with an overlying thin discontinuous membrane through a large ventral abdominal wall defect with cord insertion on top of membrane remnants.

A fetal MRI added fine details about the true size and actual content of the abdominal wall defect. As in Omphalocele cases Fig. 3, the US revealed a central large abdominal wall defect with herniation of the right hepatic lobe and a few small bowel loops through a defect with a very thin covering membrane with umbilical cord insertion on top. Fetal MRI T2WIs added herniation of

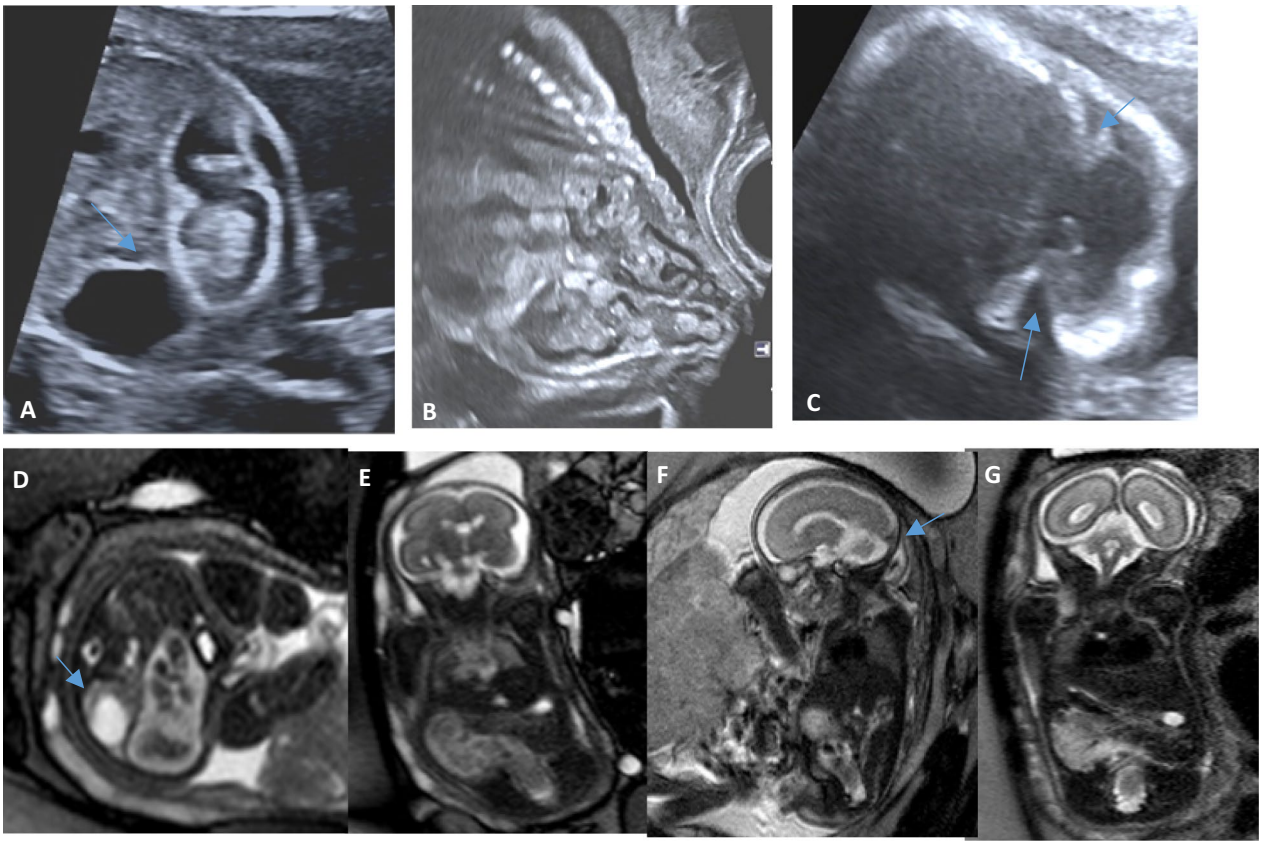

Fig. 2 A 34-year-old female 28 weeks pregnant underwent a routine 4D US revealing multiple fetal anomalies. Ultrasound findings: **A** Axial trans-abdominal image of the fetal pelvis, **B** sagittal transvaginal image of fetal abdomen and pelvis shows the dilated sigmoid colon and rectum down to the level of the anorectal junction with absent echogenic anal dimple and multiple echogenic intra-luminal well-defined lesions (enterolith). A The image also shows a well-defined cystic structure posterior to the dilated rectum with a thin echogenic wall. **C** Axial trans-abdominal image of fetal neck revealing subcutaneous cystic lesion in the fetal nape with communication with a bony defect in the occipital bone. Fetal MRI findings: **D, E, F, G** axial, coronal, sagittal, and coronal T2WIs, respectively, revealed dilated rectum, sigmoid, and descending colon with multiple enteroliths (arrowed) within (low T2 signals oval structures) and detected narrowed rectal segment below the apex of the bladder (low type). **D** The axial image revealed a low T2 signals of a cystic lesion (arrowed) posterior to the rectum (denoting calcification). **G** Coronal T2WIs revealed smooth fetal perineum with an absent anal dimple. **F** The sagittal image revealed the occipital cystic lesion. Combined US and MRI Diagnosis: Low-type anorectal malformation with recto-vesical fistula, meconium pseudocyst, and occipital encephalocele likely representing sequel of VACTERL anomaly. IUFD at GA 29 weeks

part of the fetal stomach as well as tenting of the fetal urinary bladder base while T1WIs excluded the herniation of large bowel loops owing to high meconium signals in T1WIs.

Also, in Gastroschisis cases; the US revealed herniation of a long segment of the fetal small bowel through a para-umbilical defect to the right of the umbilical cord insertion in the fetal abdomen with no overlying membrane. Fetal MRI T2WIs added the presence of thick-walled herniated bowel denoting mesenteric venous congestion (due to large hernia content compared to the rather small defect), and again TWIs excluded herniation of the large bowel loops.

Fetal abdominal cysts and masses (5 cases)

Two cases of fetal mesenteric cysts, one case of fetal ovarian cyst, one case of encysted ascites with hydrops fetalis, and one case of sacrococcygeal teratoma were included in our study. Their diagnoses were confirmed postnatally by imaging in live births and autopsy in stillbirth and IUFD. In this category, fetal MRI was superior to the US owing to its greater soft tissue characterization enabling accurate delineation of lesions and their relation to surrounding structures.

In fetal mesenteric cysts Fig. 4: prenatal US revealed well-defined thin-walled cystic lesions with clear anechoic fluid. They are either in the right upper quadrant or both left upper and lower quadrants. The US excluded their genitourinary and biliary origin. Fetal MRI T2WIs confirmed the US findings and excluded the cyst

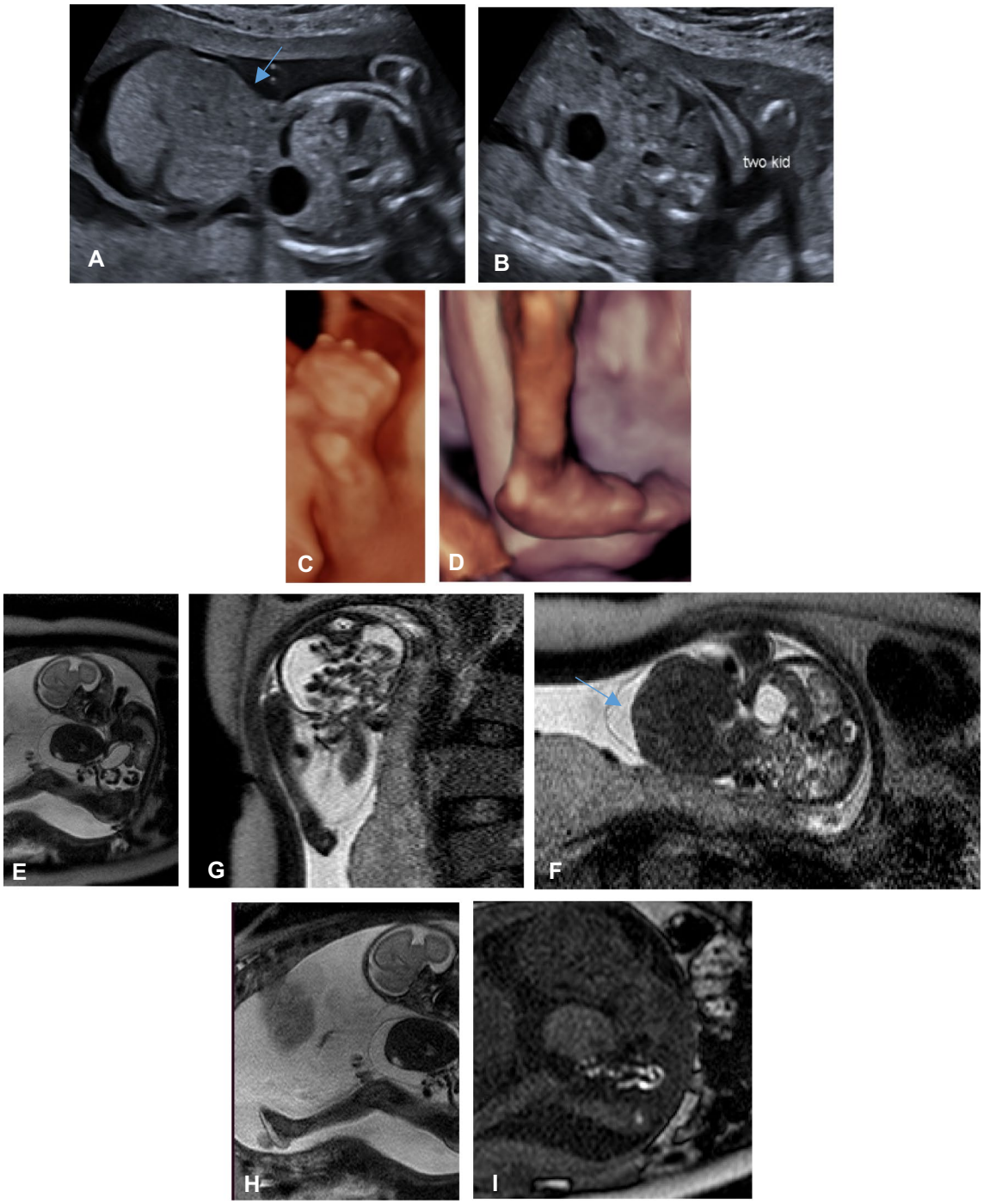

Fig. 3 A 26-year-old pregnant female with a routine 2nd trimester 4D US showing large ventral abdominal wall defect. Ultrasound findings (**A**), **B** axial sections of the fetal abdomen show a large central abdominal wall defect with herniation of the right hepatic lobe and bowel loops through. **C**, **D** sagittal 4D images revealing clenched hands and rocker bottom feet deformity. MRI findings: **E**, **H** sagittal T2WIs showing herniated liver and small bowel loops with an overlying thin membrane and associated rocker bottom feet. **F**, **G** axial T2WIs showing the size of the hernia defect, content as well as clenched hand. **I** sagittal T1WIs showing meconium signals within herniated bowel distal ileal loops. Diagnosis: The combination of skeletal anomalies with large Omphalocele suggested underlying chromosomal abnormality and trisomy 18 was diagnosed by postnatal chromosomal analysis. Termination by C.S. at 37 weeks

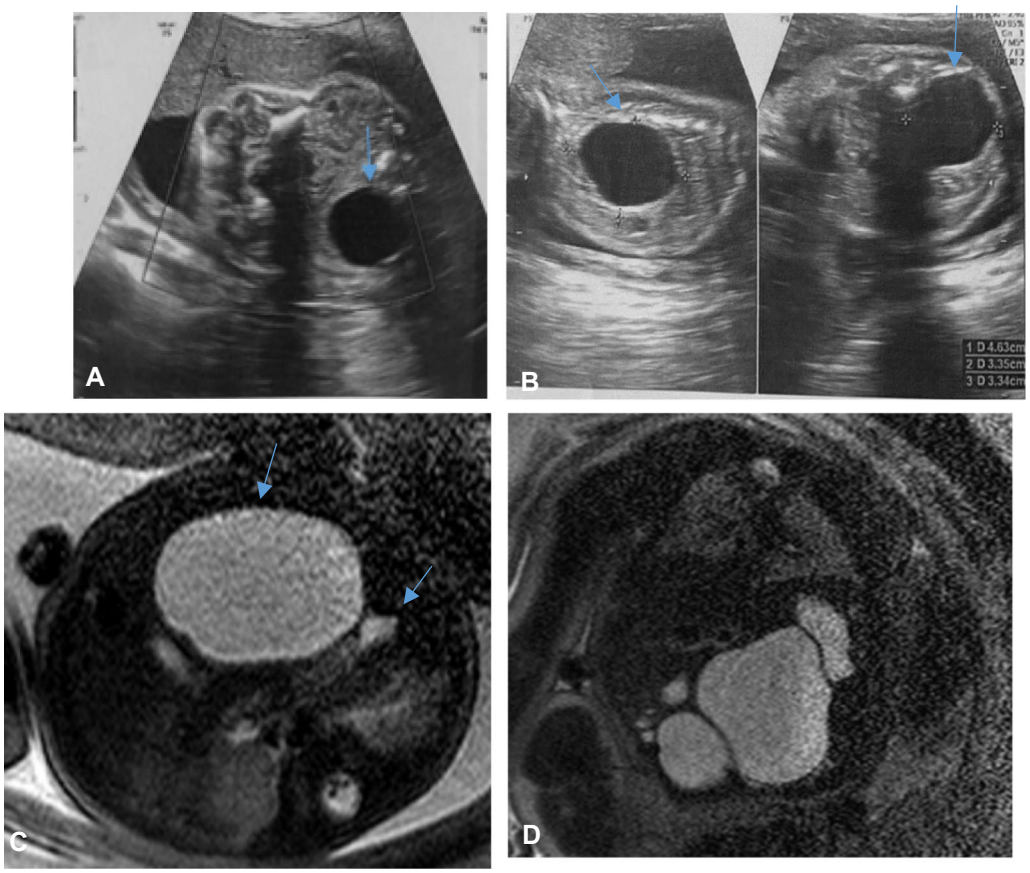

Fig. 4 A 33-year-old pregnant female with antenatal US showing a well-defined cystic structure in the fetal abdomen in the early 3rd trimester. Ultrasound findings: **A**, **B** Axial, sagittal, and axial sections of the fetal abdomen show well-defined hypoechoic cystic lesion at the right hypochondrium. MRI findings: US **C** axial T2WI, **D** coronal T2WI of fetal abdomen and pelvis revealed a well-defined cystic structure located in the right hypochondriacal and lumbar space with fluid signals within, compressing and displacing the stomach to the left side and abutting the visceral surface of the liver. MRI excluded its communication with the Gall bladder and surrounding bowel loops. Combined US and MRI Diagnosis: Large fetal mesenteric cyst. Termination by vaginal delivery at GA 39 weeks

communication with any segment of the fetal bowel as well suggesting their mesenteric origin.

In our prenatally diagnosed fetal ovarian cysts cases, prenatal US detected the presence of a left-sided unilocular anechoic pelvic cyst in a female fetus and fetal MRI confirmed the US finding and excluded its urinary and bowel origin.

In cases with ascites and hydrops fetalis, the US suspected the presence of encysted fluid around the fetal liver and free fluid in all other quadrants together with diffuse subcutaneous edema and bilateral pleural effusion. On the other hand, fetal MRI T2WIs excluded the presence of septations within the fetal abdominopelvic free fluid and confirmed the other US findings.

In cases of sacrococcygeal teratoma Fig. 5, prenatal US in the early 2nd trimester detected the presence of fetal lower back large mixed solid and cystic vascular mass lesion located at the lower lumbar and sacral regions with posterior neural element bony defect and a herniated intra-spinal lesional component. A complimentary fetal MRI was done twice (at 19 and 26 weeks). The 2nd MRI session was additive in the detection of an additional intra-pelvic extension, thus upgrading the tumor extension, and the actual size of the herniated intra-spinal components was precisely determined. Also, the prediction of complicated fetal hydrops was done owing to extensive humoral neovascularization (appearing as multiple signal void structures within the tumor) and resultant volume overload-induced heart failure.

Congenital diaphragmatic hernia Fig. 6

The antenatal US detected and measured the diaphragmatic defect. Also, the herniated small bowel and stomach to hemithorax, the liver diaphragm ratio, as well as fetal lung volume (except in two cases owing to unfavorable fetal lie) were measured. Yet, the US was limited in the detection of large bowel loops and hernia capsules.

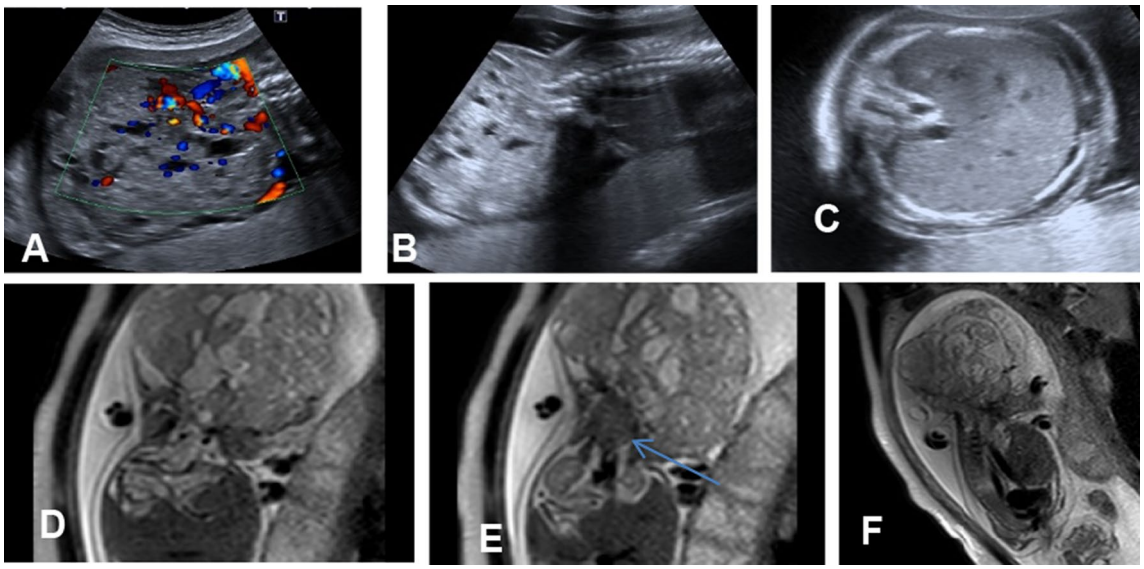

Fig. 5 A 22-year-old pregnant female with late 1st trimester and another early 2nd trimester US revealing large fetal sacral mass lesion. Ultrasound findings: **A**, **B** Axial and coronal sections of the fetal lower back showing a large mixed solid and cystic mass lesion arising from the fetal sacral region with small intra-spinal extension and extensive neovascularization on Doppler interrogation. **C** Axial image at the level of fetal liver revealing marked skin thickening and subcutaneous edema. MRI findings: **D**, **E**, **F** axial, and sagittal T2WIs revealing the mixed solid and cystic sacral mass lesion with its smaller pelvic extension (arrowed) at the level of the fetal urinary bladder and actual size of intra-spinal extension (arrowed). Note associated diffuse fetal subcutaneous edema. Combined US and MRI Diagnosis: A large mixed solid and cystic highly vascular fetal sacrococcygeal teratoma with a smaller intra-pelvic and intra-spinal extension (stage IV) and complicated fetal hydrops. IUFD at 30 weeks

Fetal MRI was additive in this category and helped in the prediction of postnatal outcome (live birth or stillbirth) as well as the post-surgical survival rate of the fetus as follows;

a. Delineating the presence of hernia capsule owing to the good definition of hernia content on T2WIs. In four out of eight cases, their hernia capsule was delineated.
b. In the setting of herniation of the liver (n = 2) (owing to a rather hyperintense signals of liver tissue on T1WIs and hyperintense signals of the portal vein and hepatic arteries on T2WIs), MRI was additive in the diagnosis of the resultant complicated herniated liver. The hepatic congestion was reported by differential hyper-intensity of the herniated liver tissue on T2WIs denoting parenchymal edema.
c. MRI was also able to detect large bowel loop herniation in six cases owing to their intra-luminal high T1 meconium signals (MR Colonography).
d. MRI was also able to accurately measure the fetal lung volume as well.

In our study, the prenatal US detected GIT anomalies in 86.1% of the studied babies, while MRI detected 96.9% of those cases who undergo fetal MRI. Table 2. Postnatal imaging or autopsy (Gold standard) of our studied GIT cases revealed their actual presence in 94.4% of the studied babies.

According to postnatal data, our prenatal ultrasound had a sensitivity of 85.3%, a specificity of 89%, a positive predictive value of 93.5%, and a negative predictive value of 96.7% for detecting congenital GIT anomalies. The diagnostic success rate was 80%. On the other hand, in our investigation, MRI had 100% sensitivity, 50% specificity, 100% positive predictive value, and 100% negative predictive value with regard to postnatal findings. There was 96.6% diagnostic accuracy. Table 3. Concerning postnatal results, our combined US and MRI had a 100% sensitivity, 89% specificity, 93.1% positive predictive value, and 96.7% negative predictive value for detecting congenital GIT anomalies. There was 93.1% diagnostic accuracy. Table 3.

Discussion

During the abnormalities screening ultrasound examination, aberrant pictures or the absence of normal structures are used to diagnose fetal abdominal malformations. Therefore, it is extremely important to collect and record standard normal photographs of the abdomen (1.). For many years, ultrasound (US) has been the go-to imaging technique for prenatal diagnosis of fetal abnormalities. Prenatal ultrasonography and fetal magnetic resonance imaging (MRI) are regarded as complementary

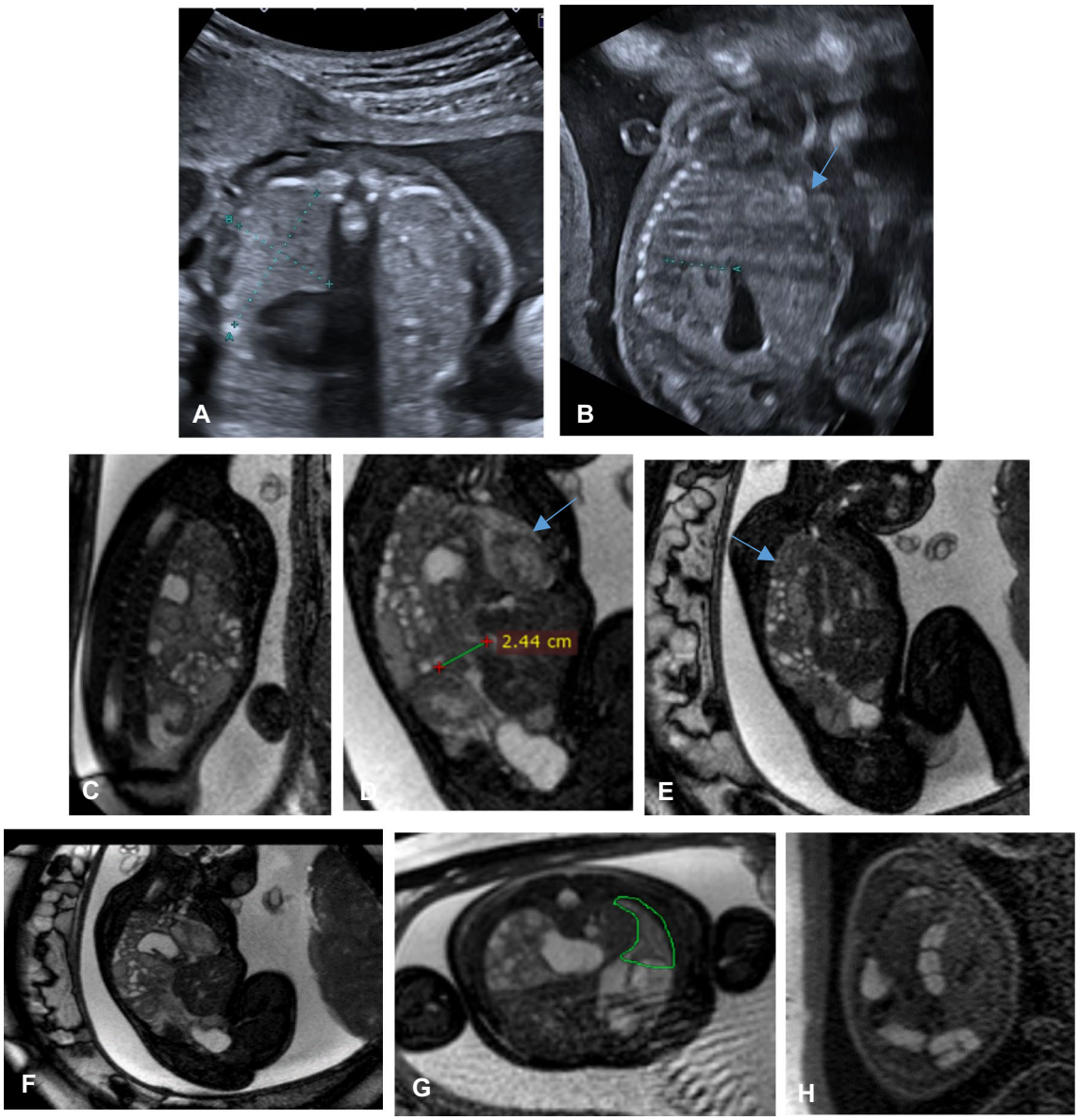

Fig. 6 A 39-year-old pregnant female with antenatal US showing large congenital diaphragmatic hernia. Ultrasound findings: **A, B** Axial and coronal sections of the fetal abdomen and chest showing left diaphragmatic hernia with herniation of the stomach and bowel into chest. MRI Findings: **C, D, E** sagittal T2WI, B coronal T2WI, and E axial T2WIs showing a large left-sided rather posterior diaphragmatic defect with herniation of the whole stomach, small bowel loops, and left hepatic lobe into whole left hemithorax with consequently marked compression of the left lung, shift and compression of heart to the left side with compressed right lung (arrowed). **F** sagittal TWI showing high meconium signal within herniated colon into the left hemithorax. Combined US and MRI Diagnosis: Large left-sided intra-pleural hernia with marked mass effect on both lungs and heart with concluded poor postnatal survival rates. Termination by C.S at GA 37 weeks

diagnostic modalities for complex fetal abdominal abnormalities [3].

In our study, we highlighted the additive role of the MRI to the routinely made prenatal US in GIT/abdominal wall anomalies. AS fetal MRI was capable of accurate delineation of the level of small bowel obstruction and differentiation of complete obstruction from luminal stenosis. Also, T1 was surprisingly suggesting the diagnosis of congenital chloride diarrhea in one case by the absence of meconium. In suspected esophageal atresia, T2 images added the presence of a distended oropharynx in one out of 2 cases. Fetal MRI added fine details about the true size and actual content of the abdominal wall defect as well as any

Table 2 Postnatal imaging or autopsy

	N **= 36**
US	
Detected	31 (86.1%)
Not detected	5 (13.9%)
MRI (*n* = 27)	
Detected	28(96.6%)
Not detected	1 (3.4%)

Table 3 Accuracy of antenatal US and MRI in the detection of congenital GIT anomalies with reference to postnatal findings among our studied group

	Postnatal findings		
	Anomaly detected	**No anomaly**	**Total**
Us findings			
Anomaly detected	29 (TP)	2 (FP)	31
No anomaly	5 (FN)	0 (TN)	5
Total	34	2	36
MRI findings			
Anomaly detected	27 (TP)	1 (FP)	28
No anomaly	0 (FN)	1 (TN)	1
Total	27	2	29
Combined US and MRI findings			
Anomaly detected	27 (TP)	2 (FP)	29
No anomaly	0 (FN)	0 (TN)	0
Total	27	2	29

TP: true positive, FP: false positive, TN: true negative, FN: false negative

related complication to the herniated organs. Also, MRI excluded the presence of septations within the fetal abdominopelvic free fluid in cases of abdominal cysts. And, the detection of an additional intra-pelvic, intra-spinal extension in the setting of SCT. In the setting of congenital diaphragmatic hernia, fetal MRI was additive in this category and helped in the prediction of postnatal outcome (live birth or stillbirth) as well as the post-surgical survival rate of the fetus.

Congenital obstructive gastrointestinal anomalies were the most frequently encountered in our study, representing 50% of our studied cases. This is agreed with both studies by Werner and Tonni [4] and Cassart et al. [7] who reported approximately similar incidences of 48 and 46%, respectively, of obstructive gastrointestinal anomalies among other studied groups of fetal abdominal anomalies.

We were in line with Furey et al. [8] and Fukuta et al. [9] on the diagnosis of fetal small bowel obstruction by the presence of three major US findings, namely the presence of dilated stomach, a dilated segment of small bowel loops and polyhydramnios. Also in those cases, fetal MRI was supplementary to the US in confirmation and accurate delineation of the level of small bowel obstruction. This coincides with the fetal MRI stated significance by He et al. [10] in their cases of small bowel obstruction. Fetal MRI in our study also helped in the differentiation of complete obstruction from luminal stenosis. Fukuta, et al. [9] and Li et al. [11] highlighted this differentiation as a major additive value of fetal MRI to the prenatal US.

High T1WIs meconium signals was particularly useful in our studied group of small bowel obstruction as it aided in the separation of jejunal atresia from ileal atresia and also in the exclusion of multiple stenotic bowel segments. He et al. [10] and Liana and Lesnic [1] also used this characteristic sign in their study as an advantage to the US to exclude multiple stenotic bowel segments which had a great effect on postnatal and post-surgical survival rates of their studied infants.

Silva et al. [12] stated that late 3rd trimester isolated fetal bowel dilatation may be connected to a different postnatal outcome where some of their studied cases presented with late small bowel dilatation with no associated polyhydramnios and on their postnatal evaluation was free of any intestinal anomalies. This presumption agreed with the outcome of our suspected cases of ileal obstruction in the late 3rd trimester which was born normally and postnatal erect abdominal X-ray showed no sign of bowel dilatation or obstruction questioning the isolated value of bowel dilatation in the late 3rd trimester in accurate diagnosis of small bowel obstruction. This questioning partially disagreed with Furey et al. [8] who considered that fetal bowel dilatation is an important sonographic and MRI sign of small bowel obstruction.

The characteristic double bubble sign of duodenal atresia stated as US and MRI diagnostic sign by Furey et al. [8] and Li et al. [11] was encountered in our US-diagnosed cases of complete duodenal atresia coinciding with its significance.

Anorectal malformations as a separate subgroup were diagnosed by prenatal US in our study depending on the presence of dilated rectal pouch with suspected stenosis/obstruction of distal rectum together with dilated small bowel loops and polyhydramnios which agreed with US diagnostic criteria of anorectal malformations stated by Podberesky et al. [13] and Rohrer et al. [2]**.** T1WI was again particularly useful in this subgroup as they delineated the abnormality in the rectal caliber and meconium signal and showed the relation between the rectal pouch and urinary bladder and this coincided with the significance of MR colonography in cases of anorectal malformations stated by Podberesky et al. [13].

The associated recto-vesical fistula was concluded in one of the cases due to the presence of echogenic partially calcified well-defined structures within the distended rectal pouch on the US and low signals intensity structures in the fetal rectum on T2WIs which agreed with Masseli et al. [5] who claimed that in cases of recto-vesical fistulae, urine from the fetal bladder fills the rectal pouch and mixes with the meconium, which precipitates into intra-luminal calcifications, also known as enteroliths, and is used as an indirect sign of the condition. The PH of the fetal bowel mostly was the main cause of this condition.

Fetal MRI was able to accurately diagnose our case of congenital chloride diarrhea owing to the absence of intrinsic high T1 signals of meconium on T1WIs being replaced by low T1WIs signals (fluid signals). Dimitrov et al. [14] and Kawamura et al. [15] also stated that fluid in the colon replacing the expected meconium together with dilated small bowel loops strongly suggests the underlying congenital chloride diarrhea.

We and Garabeclian et al. [16] agreed on the diagnosis of esophageal atresia (EA) by a combination of the persistent small-sized/absent stomach and early 2nd trimester polyhydramnios. Yet, both US and MRI failed to detect pouch signs in the fetal neck in our study. This partially agreed with. Werner and Tonni [17] considered that a combination of a small/absent fetal stomach together with a pouch sign increases the likelihood of an accurate diagnosis of EA.

T2WIs of the fetal head and neck also added the presence of dilated oropharynx as an additional finding in EA cases which agreed with Werner and Tonni [17] who stated that dilated hypopharynx aids as a secondary sign in the diagnosis of EA cases.

In the category of Ventral abdominal wall defects, fetal MRI added fine details to the size, content of the defect, and presence of complications which aided in the postnatal management of these cases. Victoria et al. [18] and Masseli et al. [5] the prognostic assessment of Gastroschisis with intestinal atresia or of complications of Omphalocele looked to be commonly employed by MRI, enabling better prenatal care and parental counseling.

Differentiation of Omphalocele from Gastroschisis in our study depended on two major findings, namely the presence of an overlying membrane and its relation to cord insertion. Adams et al. [19] and Nakagawa et al. [20] also used these two major findings in their differential diagnosis of the type of ventral abdominal wall defect.

In the case of Gastroschisis, fetal MRI elaborated the presence of thick-walled herniated bowel loops with characteristic "peel sign" described by Mărginean et al. [21] to be a result of venous congestion brought on by restriction of the mesentery and an inflammatory reaction brought on by exposure to intestinal waste products in amniotic fluid. T1-weighted fetal MRI was also able to detect the presence of herniated large bowel loops owing to high meconium signal within which agreed with Victoria et al. [18]. He claimed that because meconium in the intestine is hyperintense on T1WI, it can be used to tell the gut apart from the umbilical cord.

In our study, the US-diagnosed cases of ruptured Omphalocele owing to the presence of herniated liver with an overlying thin discontinuous membrane which coincided with Adams et al. [19]. He noted that while extruded liver may be visible in a ruptured Omphalocele, extracorporeal liver is rarely seen in cases of Gastroschisis.

The presence of a short umbilical cord with fetal organs attached to the placenta as well as severe limb and spine anomalies were stated by Winkle, et al. [22] and Leyder et al. [23] as cornerstones for the diagnosis of limb body wall defect. Such major findings were all detected in our studied four cases of body stalk anomaly coinciding with their significance.

As regards fetal abdominal cysts and masses, fetal MRI was superior to the US owing to its greater soft tissue characterization enabling accurate delineation of lesions and their relation to surrounding structures. That was in line with the conclusions of Nemec et al. [24], who claimed that prenatal magnetic resonance imaging (MR) has been shown to be useful in the identification, characterization, and precise examination of the extent of different abdominal cysts and complements the role of sonography.

Fetal MRI was very useful in the accurate detection of the true size of the intra-spinal component and in the detection of intra-pelvic extent of the sacrococcygeal teratoma which affirmed the findings of Hedrick et al. [25], who said that fetal MRI was superior to sonography in determining the intra-pelvic and intra-spinal extent of malignancy, allowing for better perinatal care. Owing to large tumor size and the presence of extensive neovascularization, our studied case ended with IUFD in 2nd trimester which coincided with Victoria et al. [18] stated that fetuses with tumors that are primarily cystic and avascular in appearance have a better prognosis than fetuses with tumors that are generally solid and highly vascularized.

Compared to the US, fetal MRI was more effective at diagnosing congenital diaphragmatic hernia (CDH) in our study by its ability in differentiating points between capsulated hernias and free hernias, detect the resultant complicated hepatic congestion, and accurately measure the fetal lung volume to detect CDH associated with fetal lung hypoplasia. Those advantageous findings of MRI were reported by studies by Victoria et al. [18],

Meholin-Ray et al. [26], Spaggiari et al. [27], and Daltro et al. [28], respectively.

The sensitivity of ultrasound to detect congenital anomalies with reference to postnatal findings was 85.3% and the specificity was 89% which was lower than the sensitivity of 96.3% and specificity of 95% stated by Rohrer et al. [2]. The US had a positive predictive value of 93.5% and a negative predictive value of 96.7%, both of which are higher than the country's declared positive predictive value of 69.7% and negative predictive value of 96%. Meholin-Ray et al. [26] in their studied group. The diagnostic accuracy of the US was 80.6% which was lower than the accuracy stated by Chalouhi et al. [29] to be 94.3%.

The sensitivity of MRI to detect congenital anomalies with reference to postnatal findings was 100%, and the specificity was 50% which was much higher than its sensitivity of 78% and nearly equal specificity of 48.6% stated by Daltro et al. [28]. The positive and negative predictive values of MRI were 100% and 100%, respectively, which is much higher than their respective values of 74.3% and 65.4%, as reported by Victoria et al. [18].

In relation to postnatal results, the combined US and MRI had a 100% sensitivity, 89% specificity, 93.1% positive predictive value, and a 96.7% negative predictive value for detecting congenital abnormalities. Diagnostic precision was 93.1%, which was consistent with Chalouhi et al. [29], Liana and Lesnic [1], and Hedrick et al. [25] that combined the US and MRI was more valuable in the detection of fine details of complex abdominal anomalies which aided in their postnatal management compared to the US alone.

The limitations of this study are the relatively small number of patients.

Conclusions

Fetal MRI is a valuable supplementary study to the prenatal US in accurate diagnosis of fetal obstructive gastrointestinal anomalies, ventral abdominal wall anomalies, fetal abdominal cysts, masses, and congenital diaphragmatic hernia**.** Fetal MRI is equally sensitive to prenatal US in anorectal malformations.

Abbreviations

2D, 3D, 4D	Two, three, four dimensional.
ADC	Apparent diffusion coefficient.
BFFE	Balanced fast field echo.
B-SSFP	Balanced steady-state fast precession.
BWS	Beckwith–Wiedemann syndrome.
CCD	Congenital chloride diarrhea.
CDH	Congenital diaphragmatic hernia.
CMV	Cytomegalovirus.
CNS	Central nervous system.
CS	Cesarean section.
DWI	Diffusion weighted images.
EA	Esophageal atresia.
ENS	Enteric nervous system.
FGR	Fetal growth restriction.
FLAIR	Fluid attenuation inversion recovery.
FSE	Fast spin echo.
GA	Gestational age.
GALD	Gestational alloimmune liver disease.
GIT	Gastrointestinal tract.
IBM	International business machine.
IUFD	Intra-uterine fetal death.
LHR	Lung to head ratio.
MCA	Middle cerebral artery.
MP	Meconium peritonitis.
MRI	Magnetic resonance imaging.
NVD	Normal vaginal delivery.
OEIS	Omphalocele, exstrophy, imperforate anus, spinal defect.
PCR	Polymerase chain reaction.
RARE	Rapid acquisition with relaxation enhancement.
SAR	Specific absorption rates.
SCT	Sacrococcygeal teratoma.
SSFP	Steady-state free precession.
SSFSE	Single-shot fast spin echo.
STIR	Short tau inversion recovery.
TAM	Transient abdominal myelopoiesis.
TFE	Turbo field echo.
TFLV	Total fetal lung volume

Acknowledgements

We thank all the participants and colleagues who provided insight and expertise that greatly assisted the research. We are also grateful for the comments offered by the anonymous peer reviewers

Author contributions

SB and HM analyzed and interpreted the patient data regarding the prenatal ultrasonographic findings. ST, HG, and MA analyzed and interpreted the patient data regarding the prenatal MRI findings. MA analyzed and interpreted the patient data regarding the postnatal findings. HM and SB revised all the data interpreted by other authors. All authors read and approved the final manuscript. All authors agreed with the content and all gave explicit consent to submit.

Funding

No funding was obtained for this study.

Availability of data and materials

The datasets used and/or analyzed during the current study are available from the corresponding author on reasonable request.

Declarations

Ethics approval and consent to participate

The current study had been approved by Kasr Al-Aini Hospital, Research and Ethical committee. We obtained IRB approval from Kasr Al-Aini committee at Cairo University. Informed written consent was obtained from all individual participants included in the study. The committee's reference number is not applicable.

Consent for publication

The authors affirm that human research participants provided written informed consent for publication of the images in the figures.

Competing interests

The authors have no relevant financial or non-financial interests to disclose.

Author details

[1]Radiology Department, Faculty of Medicine, Cairo University, 1 Kasr ELainy Street From Elkalig, Cairo, Egypt. [2]Obstetrics and Gynecology Department, Faculty of Medicine, Cairo University, 1 Kasr ELainy Street From Elkalig, Cairo, Egypt.

Received: 19 December 2022 Accepted: 20 February 2023
Published online: 24 March 2023

References

1. Liana P, Lesnic A (2018) Congenital abdominal anomalies. Congenital anomalies: from the embryo to the neonate. vol 12, pp 247–270. https://doi.org/10.5772/intechopen.69423
2. Rohrer L, Vial Y, Gengler C et al (2020) Prenatal imaging of anorectal malformations—10-year experience at a tertiary center in Switzerland. Pediatr Radiol 50(1):57–67
3. Matos APP, Duarte LDB, Castro PT et al (2018) Evaluation of the fetal abdomen by magnetic resonance imaging. Part 1: malformations of the abdominal cavity. Radiol Bras 51:112–118
4. Werner H, Tonni G (2017) Prenatal diagnosis of Beckwith-Wiedemann Syndrome Using 3D Ultrasound and Fetal MRI. In: Prenatal diagnosis of orofacial malformations. vol 2017, pp 205–209
5. Masselli G, Cozzi D, Ceccanti S et al (2021) Fetal body MRI for fetal and perinatal management. Clin Radiol 76(9):708-e1
6. Dawson B. Trapp RG (2004) Basic & clinical biostatistics. Fourth edition. 2004. 438 p. graf. SN– 9780071781329
7. Cassart, M. (2018) Urogenital fetal imaging: US and MRI. In: Pediatric urogenital radiology vol 2, pp 151–166. SN: 978-3-319-39200-4. https://doi.org/10.1007/978-3-319-39202-8_8
8. Furey EA, Bailey AA, Twickler DM (2016) Fetal MR imaging of gastrointestinal abnormalities. Radiographics 36(3):904–917
9. Fukuta A, Inoue T, Kawakubo N et al (2020) Congenital intestinal atresia associated with a mesenteric cystic lymphangioma in a low birth weight neonate: a case report. Int J Surg Case Rep 75:136–139
10. He F, Yin Y, Huang L, Li et al (2018) Using prenatal MRI to define features of meconium peritonitis: an overall outcome. Clin Radiol 73(2):135–140
11. Li X, Zhao Z, Li X et al (2020) Appearance of fetal intestinal obstruction on fetal MRI. Prenat Diagn 40(11):1398–1407
12. Silva P, Reis F, Alves P et al (2015) Fetal bowel dilatation: a sonographic sign of uncertain prognosis. Case Rep Obstet Gynecol 2015:1–4
13. Podberesky DJ, Towbin AJ, Eltomey et al (2013) Magnetic resonance imaging of anorectal malformations. Magn Reson Imag Clin 21(4):791–812
14. Dimitrov G, Bamberger S, Navard C et al (2019) Congenital sodium diarrhea by mutation of the SLC9A3 gene. Eur J Med Genet 62(10):103712
15. Kawamura T, Nishiguchi T (2017) Congenital chloride diarrhea (CCD): a case report of CCD suspected by prenatal ultrasonography and magnetic resonance imaging (MRI). Am J Case Rep 18:707
16. Garabedian C, Verpillat P, Czerkiewicz I et al (2014) Does a combination of ultrasound, MRI, and biochemical amniotic fluid analysis improve prenatal diagnosis of esophageal atresia? Prenat Diagn 34(9):839–842
17. Werner, H. and Tonni, G. (2017). Prenatal Diagnosis of Beckwith-Wiedemann Syndrome Using 3D Ultrasound and Fetal MRI. In: Prenatal diagnosis of orofacial malformations. pp 205–209. ISBN:978-3-319-32516-3. https://doi.org/10.1007/978-3-319-32516-3_19
18. Victoria T, Johnson AM, Chauvin NA et al (2011) Fetal MRI of common non-CNS abnormalities: a review. Appl Radiol 40(6):8
19. Adams AD, Stover S, Rac MW (2021) Omphalocele—what should we tell the prospective parents? Prenat Diagn 41(4):486–496
20. Nakagawa M, Hara M, Shibamoto Y (2013) MRI findings in fetuses with an abdominal wall defect: gastroschisis, omphalocele, and cloacal exstrophy. Jpn J Radiol 31(3):153–159
21. Mărginean C, Mărginean CO, Gozar L et al (2018) Cantrell syndrome—a rare complex congenital anomaly: a case report and literature review. Front Pediatr 6:201
22. Winkler NS, Kennedy AM, Woodward PJ (2012) Cloacal malformation: embryology, anatomy, and prenatal imaging features. J Ultrasound Med 31(11):1843–1855
23. Leyder M, Van Berkel K, Done E et al (2014) Ultrasound meets magnetic resonance imaging in the diagnosis of pentalogy of Cantrell with complete ectopy of the heart. Gynecol Obstet 4(200):2161–0932
24. Nemec U, Nemec SF, Bettelheim D et al (2012) Ovarian cysts on prenatal MRI. Eur J Radiol 81(8):1937–1944
25. Hedrick HL, Flake AW, Crombleholme TM et al (2004) Sacrococcygeal teratoma: prenatal assessment, fetal intervention, and outcome. J Pediatr Surg 39(3):430–438
26. Mehollin-Ray AR, Cassady CI, Cass DL et al (2012) Fetal MR imaging of congenital diaphragmatic hernia. Radiographics 32(4):067–1084
27. Spaggiari E, Faure G, Rousseau V et al (2015) Performance of prenatal diagnosis in esophageal atresia. Prenat Diagn 35(9):888–893
28. Daltro P, Werner H, Gasparetto TD et al (2010) Congenital chest malformations: a multimodality approach with emphasis on fetal MR imaging. Radiographics 30(2):385–395
29. Chalouhi GE, Millischer AÉ, Mahallati H et al (2020) The use of fetal MRI for renal and urogenital tract anomalies. Prenat Diagn 40(1):100–109

Publisher's Note